Available online at www.sciencedirect.com
ScienceDirect
Hydrometallurgy 89 (2007) 337–345
hydrometallurgy
www.elsevier.com/locate/hydromet

Kinetics of sulphuric acid leaching of a zinc silicate calcine

A.D. Souza [a], P.S. Pina [b], E.V.O. Lima [b], C.A. da Silva [b], V.A. Leão [b,*]

[a] *Votorantim Metais Zinc. BR 040, Km 284 — CEP 39205-000, Três Marias, MG, Brazil*
[b] *Núcleo de Valorização de Materiais Minerais — Department of Metallurgical & Materials Engineering, Campus Morro do Cruzeiro, s.n. 35400-000, Ouro Preto, MG, Brazil*

Received 30 May 2007; received in revised form 9 August 2007; accepted 17 August 2007
Available online 23 August 2007

Abstract

Recent developments of acid leaching and solvent extraction of zinc silicate ores have produced renewed commercial interest. However, the leaching kinetics of these concentrates has received little attention. This work, therefore, addresses the leaching of a zinc silicate concentrate in sulphuric acid. The effects of particle size (0.038–0.075mm), temperature (30–50°C) and initial acid concentration (0.2–1.0mol/L) were studied. The results show that decreasing the particle size while increasing the temperature and acid concentration increase the leaching rate. As leaching occurs, there is a progressive dissolution of willemite while the quartz and iron-containing phases remain inert. Among the kinetic models of the porous solids tested, the grain model with porous diffusion control successfully described the zinc leaching kinetics. The model enabled the determination of an activation energy of 51.9 ± 2.8kJ/mol and a reaction order of 0.64 ± 0.12 with respect to sulphuric acid, which are likely to be a consequence of the parallel nature of diffusion and chemical reaction in porous solids.

Keywords: Zinc silicate; Willemite; Kinetics; Sulphuric acid; Grain model

1. Introduction

Non-sulphide zinc deposits are genetically classified into two categories. One is the supergene deposits, derived from zinc sulphides. The other class is formed by the so-called hypogene deposits, recognized as non-sulphide zinc minerals formed by willemite or a willemite–franklinite–zincite–gahnite association. The recent developments of acid leaching (Votorantim, Brazil) and solvent extraction (Tecnicas Reunidas, Spain) of zinc silicate concentrates have produced renewed commercial interest in these ores. Within the foreseeable future, the annual production of zinc from non-sulphide sources could exceed 10% of global metal production (Boni, 2005). Accordingly, Votorantim Metais Zinc (VMZ) has devised an integrated process to treat both zinc sulphides and silicates (Souza et al., 2007). The process consists of the leaching of zinc silicate ores (willemite, Zn_2SiO_4, and hemi-morphite, $Zn_4Si_2O_7(OH)_2{\cdot}H_2O$), in the same plant that treats zinc sulphide concentrates through the traditional RLE (roasting–leaching–electrolysis) process.

In the integrated process (Souza, 2000), as calcium and magnesium carbonates are present in the zinc concentrate, this concentrate is treated with zinc wash solution (about 45g/L Zn) to obtain a slurry. This slurry is then submitted to a step where zinc is precipitated as

* Corresponding author. Tel.: +55 31 3559 1102; fax: +55 31 3559 1561.
E-mail address: versiane@demet.em.ufop.br (V.A. Leão).

0304-386X/$ - see front matter © 2007 Elsevier B.V. All rights reserved.
doi:10.1016/j.hydromet.2007.08.005

basic zinc sulphate ($ZnSO_4 \cdot 3Zn(OH)_2 \cdot 4H_2O$, (Chen and Dutrizac, 2003)) while the magnesium remains in the sulphate solution (Eq. (1)).

$$3\ ZnSO_4 + 0.5\ Zn_2SiO_4 + 7\ H_2O + CaCO_3 + MgCO_3 \rightarrow ZnSO_4 \cdot 3Zn(OH)_2 \cdot 4H_2O + 0.5\ SiO_2 + CaSO_4 + MgSO_4 + 2\ CO_2 \quad (1)$$

Zinc is precipitated at 95°C or alternatively, at 180–200°C and 18bar pressure, so that basic zinc sulphate is readily formed (Souza, 2000). The influent wash solution is pH 5.0 and reaches pH 6.6 after neutralization by the carbonates, present in the silicate concentrate, which results in zinc precipitation from the wash solution. The basic zinc sulphate is then dissolved with 180g/L sulphuric acid, which has been returned from the electrolysis step (spent solution) of the RLE process. After thickening and filtration, the clarified solution is sent to the neutral leaching (pH 4.0) step of the RLE process, completing the integration of the sulphide and non-sulphide concentrate treatment (Souza, 2000).

Direct silicate leaching with sulphuric acid can be represented by Eqs.(2) and (3) for hemi-morphite and willemite, respectively.

$$Zn_4Si_2O_7(OH)_2 \cdot H_2O + 4\ H_2SO_4 \rightarrow 4\ ZnSO_4 + Si_2O(OH)_6 + 3\ H_2O \quad (2)$$

$$Zn_2SiO_4 + 2\ H_2SO_4 \rightarrow 2\ ZnSO_4 + Si(OH)_4 \quad (3)$$

The monosilicic acid ($Si(OH)_4$), produced in Eq. (3), polymerizes and may form particles of colloidal silica (Espiari et al., 2006). Besides, a gel is formed which is not filterable. Much effort has been applied to precipitate silica without forming a gel. Some authors have suggested the use of flocculants, such as aluminium sulphate, to remove the silica gel; while others have proposed the use of microwave radiation for the same purpose (Hua et al., 2002).

The kinetics of zinc silicate dissolution is far less studied than that of zinc sulphides. Terry and Monhemius (1983) have comprehensively studied the leaching kinetics of natural hemi-morphite, as well as natural and synthetic willemite. The authors have observed that the acidic dissolution was diffusion-controlled for hemi-morphite and chemically-controlled for willemite leaching. Abdel-Aal (2000), studying the leaching kinetics of low grade zinc silicate, proposed that the process was controlled by diffusion on an "ash" layer with an associated activation energy of 13.4kJ/mol. As shown in Eqs.(2) and (3), there is no solid reaction product formed during leaching, as only zinc ions and silica gel are produced, although the latter can affect the transport properties of the solution. It should be pointed out that Abdel-Aal (2000) did not present an explanation for the proposed diffusion control in the product layer. It is also possible that diffusion through the solid's pores would explain the controls observed during silicate leaching. It has been shown that if the transport through a solid's pores is the rate-determining step, an expression similar to the shrinking core model (SCM) with diffusion control is achieved (Georgiou and Papangelakis, 1998).

This work addresses the leaching kinetics of a zinc silicate calcine which can be represented by a variant of the SCM when diffusion through the product layer is the rate-determining step.

2. Materials and methods

The zinc silicate calcine, assaying 43.5% Zn (Table 1), was produced by roasting a zinc silicate floatation concentrate in a rotary kiln at temperatures of 700–800°C, for 60min aimed at removing organic matter. XRD of the calcine showed the presence of willemite (Zn_2SiO_4) as the main zinc-containing phase and franklinite ($ZnO \cdot Fe_2O_3$) as a minor constituent. This was based on the iron content of the zinc silicate calcine (Table 2). Hematite and magnetite, as well as quartz and dolomite, constituted the gangue.

Prior to the leaching experiments, the zinc calcine was dry-ground and wet-sieved to yield a particle size distribution between 150μm and 38μm. The zinc and iron content as well as surface area, total porous volume and porous average diameter of the different sieved fractions are also depicted in Table 2. The chemical leaching tests were carried out batch-wise in a closed water-jacketed glass reactor using 500mL solution and 10g/L solids. Agitation was provided by a magnetic stirrer that enabled adequate dispersion of the mineral particles without evaporation loss of the solution. The leaching temperature was evaluated in the range of 30 to 60°C and the acid concentration between 0.2 and 1.0mol/L was studied. At selected time intervals, a small known amount (3mL) of slurry was withdrawn and quickly filtered. The first sample was taken after 30s of mixing, and 10s was required for each sampling and filtration procedure. The zinc extraction was determined by analyzing zinc concentration in solution (Atomic Absorption Spectrometry, Perkin Elmer AAnalyst 100) and for every sample taken from the reactor, the volume change was taken into account in the zinc extraction determinations, which were calculated based on the mass of zinc

Table 1
Chemical analysis of bulk zinc silicate calcine (%)

Zn	SiO_2	Fe	Cd	Cu	Co	Pb
43.50	23.30	5.90	0.01	0.003	0.003	1.25

Table 2
Zn and Fe analysis and surface area of different sized fractions of zinc silicate calcine

Size fraction	Zn (%)	Fe (%)	Surface area (m^2/g)	Total pore volume (mm^3/g)	Pore average diameter (nm)
105–75 μm	44.50	3.64	2.0	8.8	17.2
75–53 μm	46.44	3.59	2.6	8.8	13.6
53–45 μm	45.51	4.53	2.3	11.8	20.3
45–38 μm	44.48	4.48	2.5	12.9	20.7

dissolved as function of time, according to the following equation:

$$\text{Zn.extr} = \frac{[\text{Zn}]_{T_{0+T}}}{[\text{Zn}]_{T_0}} \cdot 100 \quad (4)$$

Surface area and pore volume were determined by nitrogen adsorption. Nitrogen isotherms were performed with a Nova 1000 High Speed Gas Sorption Analyzer (*Quantachrome*). Sample degassing was carried out at 80°C, for 24h, to avoid decomposition. Nitrogen adsorption was performed at − 196°C. Data were collected from a relative pressure (p/p_0) of 0.05 to 0.98. A large sample (~4.0g) was used and the Nova 1000 parameters (equilibration tolerance, time to remain in tolerance and maximum equilibration time) were set at 0.05, 360 and 720, respectively, to improve the accuracy of low surface area measurements with nitrogen adsorption.

The analyses of the silicate calcine and leaching residues were carried out by SEM–EDS. The samples were coated with graphite by electro-deposition, using a JEOL JEE 4C instrument and observed in a JEOL JSM 5510 scanning electron microscope (SEM), equipped with a spectrometer for micro-analysis based on a Energy Dispersive X-ray Spectroscopy system (EDS), and having an accelerating voltage 0.5–30kV. Electron microprobe analysis have confirmed willemite as the main zinc mineral since the metal content of different grains is similar to that of a pure mineral (theoretical, Table 3).

Statistical analysis was carried out using the Origin™ version 6.0 software. This determined both the activation energies and the order of reactions with respect to sulphuric acid–determined for a 95% confidence interval.

3. Results and discussion

3.1. Effect of agitation speed

Fig. 1 shows little effect of stirring speed on zinc dissolution in the range 360–720rpm. Therefore, the dissolution process

Table 3
EDS analysis (Zn, Si and O) of zinc silicate calcine (average of 6 points)

Element	EDS analysis	Pure willemite
Zn	55.97	58.67
Si	12.56	12.61
O	31.57	28.72

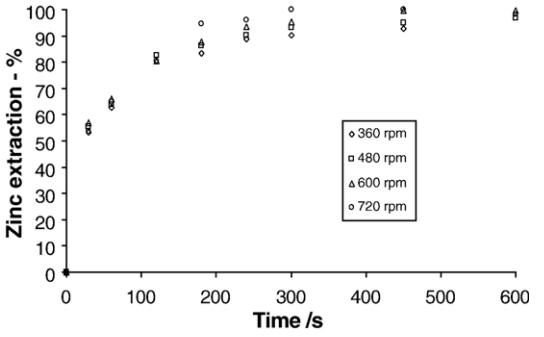

Fig. 1. Effect of stirring rate on zinc extraction. (0.4 mol/L H_2SO_4, 10 g/L solids, temperature 40 °C and particle size 75–53 μm).

does not seem to be controlled by mass transfer through the liquid boundary layer, despite the change in solution viscosity caused by the formation of silica gel. As a result, the stirring speed was kept at 480rpm, unless otherwise stated.

3.2. Effect of temperature

Fig. 2 shows the rate of zinc extraction increases significantly as a function of temperature in the range of 30–60°C. Similar results were observed by Bodas (1996) and Espiari et al. (2006), that carried out leaching experiments with a zinc silicate ore containing hemi-morphite ($Zn_4Si_2O_7(OH)_2{\cdot}H_2O$) and smithsonite ($ZnCO_3$) as major zinc minerals. Similarly, Abdel-Aal (2000) studied the leaching of a zinc silicate ore containing willemite and hemi-morphite and observed that as temperature was increased from 40°C to 70°C, zinc extraction enhanced from 70 to 95%.

3.3. Effect of sulphuric acid concentration

Fig. 3 shows that the rate of zinc extraction also increases with the sulphuric acid concentration, in the range assessed. This behaviour was previously observed by Bodas (1996), Abdel-Aal (2000) and Espiari et al. (2006), in sulphuric acid medium. Terry and Monhemius (1983) studied the effect of sulphuric, nitric, phosphoric and hydrochloric acid concentrations

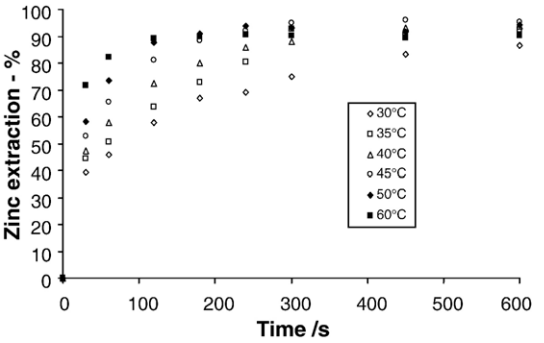

Fig. 2. Effect of temperature on zinc extraction. (0.4 mol/L H_2SO_4, 10 g/L solids, stirring rate 480 rpm and particle size 75–53 μm).

upon zinc dissolution from natural willemite samples. The authors observed that the rate of zinc dissolution was strongly dependent on both the acid (proton) concentration and the acidic anion (SO_4^{2-}, PO_4^{3-}, Cl^- and NO_3^-). The following reactivity order was observed by the authors with respect to the acid anion: $HCl \approx HNO_3 < HClO_4 < H_2SO_4 \approx H_3PO_4$. Terry and Monhemius (1983) suggested that the difference in the reactivity order was in function of the complex affinity for the zinc ion.

3.4. Effect of the particle size

The decrease in particle size enhanced zinc dissolution (Fig. 4), although the zinc extraction with a particle size between 38–45mm, is only 7% higher than that with 75–53μm particles. Usually, the literature shows that the smaller the particle size, the faster the reaction rate, as observed by Abdel-Aal (2000). The small difference observed can be likely ascribed to the negligible increase of the particle surface area (BET surface area) with decreasing particle sizes due to the porosity of the solid (Table 2). Massaci et al. (1998) also observed the insignificance of particle size on the leaching kinetics, while studying ferric sulphate leaching of a zinc sulphide ore. The authors credited this behaviour to the presence of a natural porosity in the zinc sulphide particles, but they did not present surface area and porosity analysis. The high reactivity of the roasted silicate in sulphuric acid medium associated to a small difference in the surface area of the different size fractions, could have masked the effect of particle size upon the zinc leaching rate (Aydogan et al., 2005; Bobeck and Su, 1985; Ghosh et al., 2002; Silva, 2004).

3.5. Morphology of the leaching residues

The morphology of the zinc silicate calcine particles before and after leaching was examined by SEM–EDS. The solid particles present a rough and porous surface generated by the calcination process that resulted in the sintering of the small particles found on the surface of the larger ones, as observed in the Fig. 5(a) and (b). The micrograph of the leaching residues shows a progressive increase in the roughness and porosity of the solid. For instance, after 45% zinc extraction (Fig. 5c and d), the particles present a high degree of degradation, that sharply increases along the progress of dissolution (Fig. 5e and f). In spite of the surface degradation generated by the leaching process, Fig. 5(a–f) suggest that the particle surface does not present a reaction product layer. Notwithstanding, as shown in the XRD patterns (Fig. 6) of the zinc silicate and the leaching residues (after 1 and 3min), willemite is selectively leached, while the quartz and iron-containing phases (hematite and magnetite) remain as an "ash" layer. Therefore, it is proposed that the zinc dissolution process be controlled by diffusion of the reagent in the porous structure of the calcine particles, as observed by Georgiou and Papangelakis (1998) in pressure leaching experiments carried out with limonitic laterite ores.

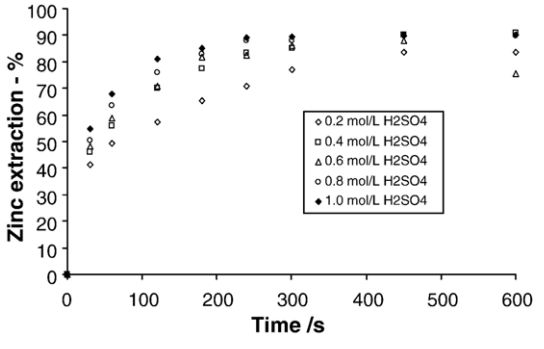

Fig. 3. Effect of acid concentration on zinc extraction (conditions as Fig. 2).

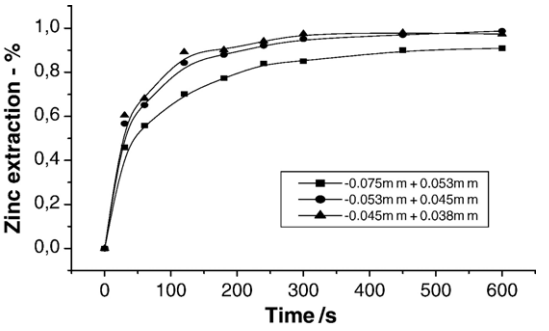

Fig. 4. Effect of particle size on zinc extraction (conditions as Fig. 2).

3.6. Kinetics analysis

The leaching of zinc silicate calcine in sulphuric acid solutions includes a heterogeneous reaction as represented by Eqs.(2) and (3).Assuming that the zinc silicate particles have a spherical geometry and the chemical reaction is the rate-controlling step, the following expression of the shrinking core model can be tested to describe the dissolution kinetics of the process:

$$1-(1-\alpha)^{\frac{1}{3}} = k_R \cdot t,\ k_R = \frac{b \cdot k \cdot [H_2SO_4]^n}{\rho_{silicate} \cdot r_0} \quad (5)$$

Similarly, when the diffusion of the reagent through a product layer is the rate-controlling step, the following expression of the shrinking core model is achieved to describe the dissolution kinetics:

$$1-3(1-\alpha)^{\frac{2}{3}}+2(1-\alpha) = k_d \cdot t \quad (6)$$

where $k_d = \frac{6 \cdot b \cdot D_{eff} \cdot [H_2SO_4]}{\rho_{silicate}}$.

According to Eqs.(5) and (6), when chemical reaction is the rate-controlling step, a plot of $[1-(1-\alpha)^{1/3}]$ versus time is a straight line with a slope k_R. Conversely, when the process is controlled by diffusion through the solid product layer, a plot of $[1-3(1-\alpha)^{2/3}+2(1-\alpha)]$ versus time is also a straight line whose slope is k_d (Levenspiel, 1999). Furthermore, for all purposes, k can be written as $k = A \cdot k_0 \cdot [H_2SO_4]^n$ where A = area of reaction; k_0 = Arrhenius pre-exponential factor; and n = reaction order.

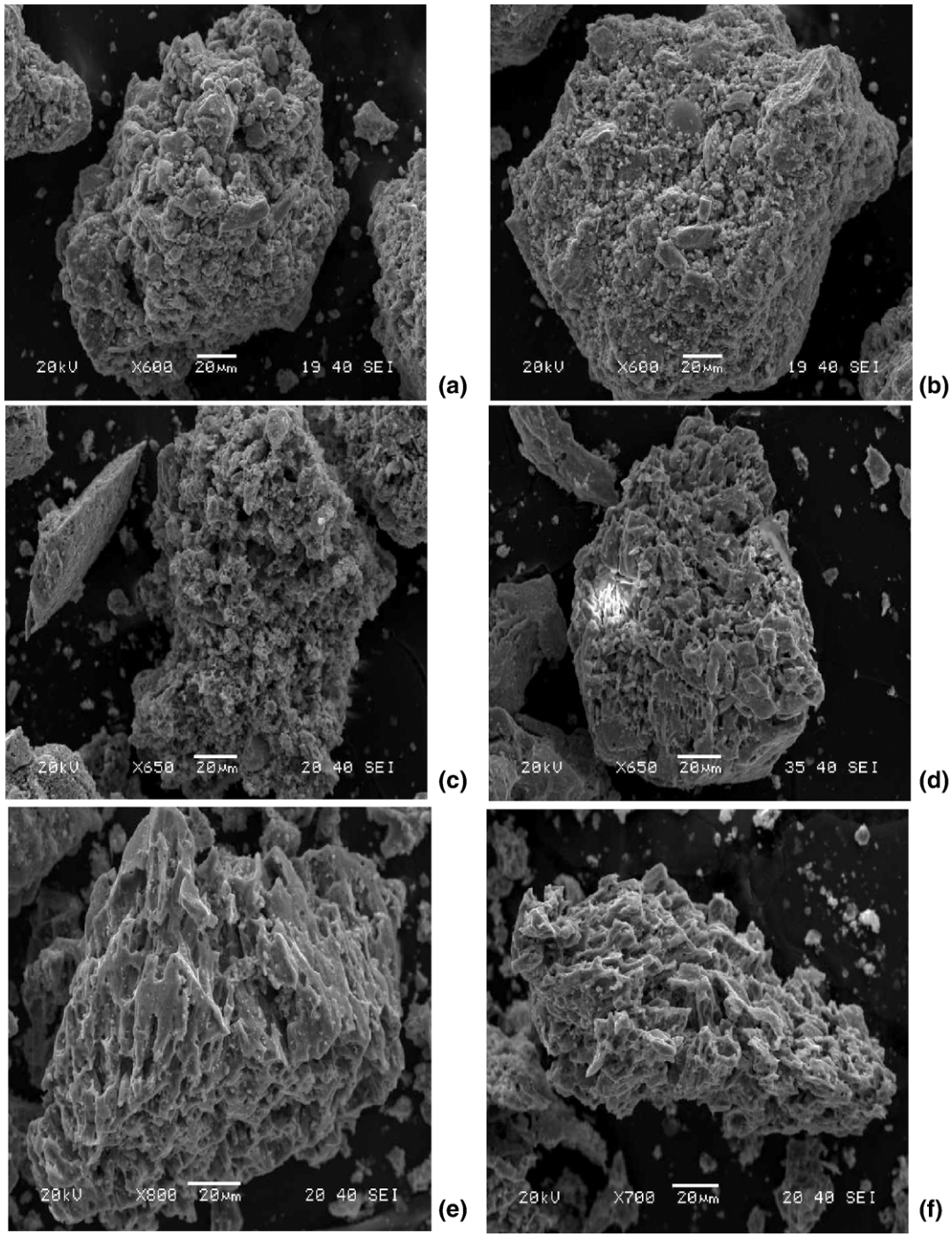

Fig. 5. 105–150 μm particles of zinc silicate calcine before leaching (a and b); after 45% Zn extraction (c and d); and after 80% Zn extraction (e and f).

Fig. 7 presents the fitting of the SCM model with chemical reaction control (Eq. (5)) and product diffusion control (Eq. (6)) to the experimental data. It is readily noted that the model for product diffusion control is better than the one for chemical reaction control. Nevertheless, the dissolution of the zinc silicate calcine occurs without the formation of a product layer, as shown in Fig. 5. Therefore, this model is not consistent with the physical picture of the process. Thus, Eq. (6) is unlikely to physically represent the reacting system and a different model, which takes into account the effect of porosity, should be tested so that the zinc silicate leaching can be adequately described. In the latter, the aqueous reactant

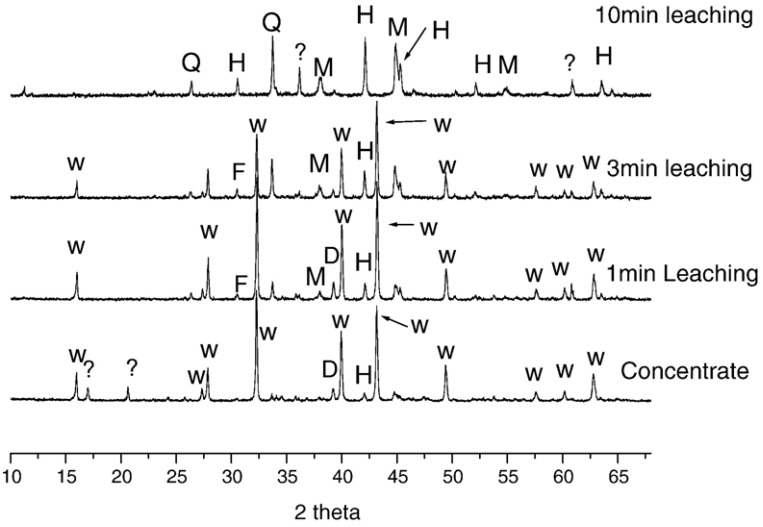

Fig. 6. XRD pattern of the zinc silicate calcine. Q: quartz, H: hematite, M: magnetite, W: willemite, F: franklinite, D: dolomite.

diffuses and reacts concomitantly so that diffusion and chemical reaction occurs in parallel, instead of in series, as predicted by the shrinking core model applied to non-porous solids (Sohn and Wadsworth, 1979).

Several models have been proposed to describe the leaching kinetics of porous solids, such as: (i) the *random pore model*, (ii) the *uniform pore model* and (iii) *the grain model*. The random pore model could not be applied to represent the leaching process as observed elsewhere (Filippou et al., 1997). The uniform pore model with chemical control was also tested to describe the leaching kinetics, but did not produce a good fit to the experimental data, as observed in other hydrometallurgical systems (Filippou et al., 1997; Raghavan and Gajam, 1986). The grain pore model will be discussed below.

Modelling porous solids leaching kinetics, Sohn and Wadsworth (1979) stated that the concentration of the reactant is uniform throughout the solid when the resistance associated to diffusion is small. If the diffusion resistance is large, conversely, the reaction occurs in a narrow layer near the external surface because the reactant cannot penetrate deeply inside the pores before reacting. Assuming that external mass transfer is fast and that this layer is much thinner than the particle dimensions, the authors proposed the following equation for the overall rate (r_i):

$$r_i = \left(\frac{2}{n+1} k S_v D_{\text{eff}}\right)^{\frac{1}{2}} [i]_s^{\frac{n+1}{2}} \tag{7}$$

In Eq. (7), k is the chemical rate constant, and therefore the overall rate is increased even when k is large (the reaction is fast). This means that diffusion alone does not control the overall rate, a consequence of the parallel nature of the chemical reaction and diffusion in porous solids (Sohn and Wadsworth, 1979). An

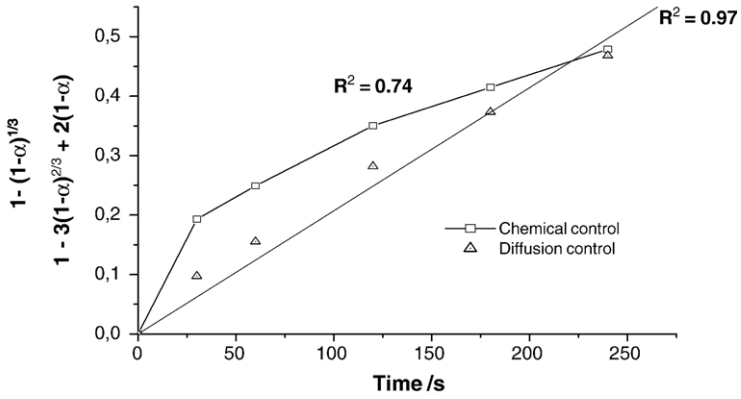

Fig. 7. Fitting of the shrinking core and grain models (conditions as Fig. 2).

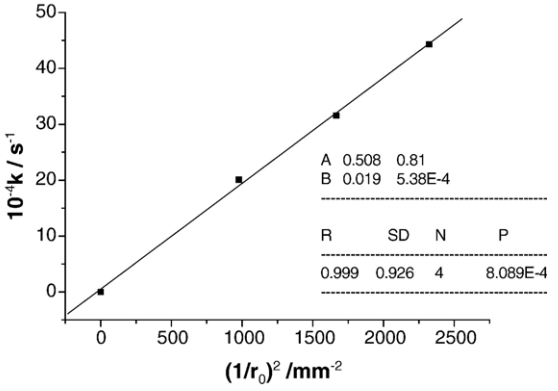

Fig. 8. Plot of k_D versus $1/r_0^2$. (In the estimated linear regression model, A and B represent the values of the intercept and slope, respectively, followed by their respective standard errors. R is the correlation coefficient; N, the number of data points and SD, the standard deviation of the fit).

important outcome of Eq. (7) is that both the activation energy and reaction order of the process are an average of the values associated with the chemical reaction and diffusion steps.

The grain model (Szekely et al., 1976) can also be applied to describe the leaching kinetics of porous solids. It considers that the solid reactant is made up of a large number of individual grains of the same size and form, which are similar to the exterior form of the particle (i.e. a spherical particle is formed by spherical non-porous grains). When the reaction is chemically-controlled, there is no resistance for diffusion throughout the pores, the fluid reactant concentration is uniform in the whole solid, and an expression similar to Eq. (5) is produced. Nevertheless, if chemical reaction resistance is negligible, as compared to that due to pore diffusion, the reaction occurs in a narrow region and this situation is similar to the shrinking core model with ash layer control, applied to nonporous solids. The model gives the following expression for spherical particles (Georgiou and Papangelakis, 1998):

$$1-3(1-\alpha)^{\frac{2}{3}}+2(1-\alpha)=\frac{t^*}{\hat{\sigma}^2} \tag{8}$$

where t^* and $\hat{\sigma}$ are defined as follows:

$$t^*=\left(\frac{bk[H_2SO_4]}{4r_0\rho_{silicate}}\right)t \tag{9}$$

$$\hat{\sigma}=\frac{r_0}{3}\left(\frac{3k(1-\varepsilon_0)}{8r_0D_{eff}}\right)^{\frac{1}{2}} \tag{10}$$

By applying Eqs.(9) and (10) to solve Eq. (8), the following expression is achieved to describe the zinc silicate leaching:

$$1-3(1-\alpha)^{\frac{2}{3}}+2(1-\alpha)=k_Dt$$

$$\text{where } k_D=\frac{3D_{eff}[H_2SO_4]}{r_0^2\rho_{silicate}(1-\varepsilon_0)}$$

As shown in Fig. 7, a good fit ($r^2 > 0.97$) is observed when the left hand of Eq. (11) is applied to the experimental data. Furthermore, from the analysis of Eq. (11), there is a clear dependence of the model constant, k_D, with the inverse square of initial particle radius ($1 / r_0^2$).

Fig. 8 presents the plot of k_D versus $1 / r_0^2$ that was obtained from the linear fitting of the data present in the Fig. 4 into Eq. (11). It can be seen from Fig. 8 that there is a linear relationship between the rate constant and the square of the inverse of the initial particle radius, $1 / r_0^2$. This behaviour supports the application of the grain model with pore diffusion control to describe the dissolution kinetics of the zinc silicate calcine.

Fig. 9 presents the Arrhenius plot constructed with the rate constant value, k_D, calculated from the data presented in Fig. 2. The activation energy determined for the pore diffusion control is 51.9 ± 2.8kJ/mol. This value is similar to those obtained by Terry and Monhemius (1983), that found 49.2kJ/mol and 39.0kJ/mol for the dissolution of natural and synthetic willemite samples in sulphuric acid solution (pH 1.90), respectively. Similarly, Espiari et al. (2006) found an activation energy of 23.5kJ/mol for the dissolution of zinc-rich tailings (smithsonite and hemi-morphite) in sulphuric acid solutions and stated that the dissolution process was controlled by an adsorption/desorption process. The value determined in the present work is high for the diffusion of ions in solution, although similar values were proposed for the diffusion-controlled leaching of other porous materials, as shown in Table 4. These values are likely derived from the parallel nature of diffusion and reaction in porous solids as shown in Eq. (7). This implies that the apparent activation energy is the average of that for intrinsic reaction and diffusion, as already stated.

When the zinc silicate leaching is diffusion-controlled, the effective diffusion coefficient, determined from Eq. (11), should be smaller than that for aqueous solutions. Table 5 presents the values for the effective diffusion coefficients of sulphuric acid as a function of the leaching temperature from 30°C to 60°C. The effective diffusion coefficient slightly increases with temperature, in the range studied in this work, as expected. Nzikou et al. (1997) determined the diffusion coefficient of sulphuric acid in higher than 0.2mol/L aqueous solutions and 25°C. According to

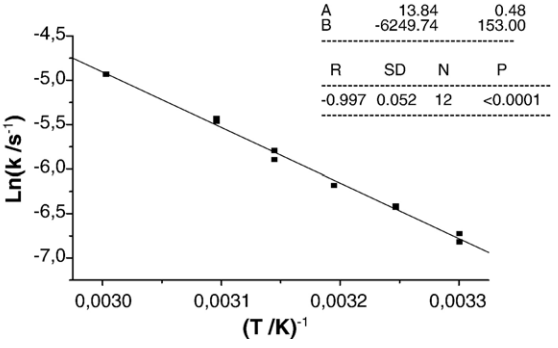

Fig. 9. Arrhenius plot for the grain model.

Table 4
Selected values of activation energies observed during the leaching of porous materials

Material leached	Experimental conditions	Activation energy (kJ/mol)	Reference
Spent nickel catalyst	10% solids, 50–90 °C, sulphuric acid	69.1	(Sahu et al., 2005)
Chalcopyrite leaching with $Na_2Cr_2O_7$	Stoichiometric amount of reactant-molybdenite concentrate	40	(Ruiz and Padilla, 1998)
Leaching of Ni smelter slag	Leaching in the presence of SO_2, 4–35 °C, 1% solids, 600 rpm	70 (for Co, Fe) 50 (for Ni)	(Gbor et al., 2000)
Niobium leaching with NaOH	30% solids, 300 g/L KOH, 150–200 °C, Nb concentrate	72.2	(Zhou et al., 2005)
Acid pressure leaching of limonite	30% solids, 230–150 °C, 64.8 m^2/g surface area, H_2SO_4/ore ratio: 0.2	85.4 (estimated)	(Georgiou and Papangelakis, 1998)

the authors, a value of 1.8×10^{-5} cm^2/s at 25°C is proposed for the diffusion of sulphuric acid in aqueous solutions, which is the same as that calculated using the equations. proposed by Umino and Newman (1997), considering that their model can be applied to a 0.4mol/L solution. Utilizing the activation energy determined in the present work, a diffusion coefficient of 1.2×10^{-7} cm^2/s was estimated at 25°C for the zinc silicate leaching, which is two orders of magnitude lower than that proposed for aqueous solutions. Similarly, the apparent reaction order with respect to sulphuric acid was 0.64 ± 0.12 (as determined from Fig. 10 and the kinetic data in Fig. 3), which is also an average for the chemical reaction and diffusion values (Sohn and Wadsworth, 1979). Summarizing, the leaching of zinc silicate is likely controlled by the transport inside the silicate pores.

The results of the present work suggest that the zinc silicate leaching is not strongly affected by the particle size, implying that fine grinding of such concentrates is not required. Therefore, a rigid control of the size reducing process is not necessary and the energy consumption during grinding could be reduced. Finally, as diffusion inside the pores is the slowest step, it is likely that an increase in the stirring speed could only marginally affect the leaching rate, as the diffusion inside the pores is not strongly affected by stirring in the bulk. Except for the practical effect of solids settling inside the reactors, a complex and expensive stirring system is not required.

4. Conclusions

The dissolution kinetics of a roasted zinc silicate (willemite) concentrate in sulphuric acid solutions was studied. It was found that the zinc extraction was fast and increased with temperature and sulphuric acid concentration. The shrinking core model with diffusion control fitted the experimental results, although it could not physically represent the leaching kinetics. The use of the grain model, which successfully described the dissolution of zinc analysis of the zinc silicate particles, is suggested because there was no reaction product on the particle surfaces. The apparent activation energy and reaction order were determined as 51.9±2.8 kJ/mol and 0.64±0.12, respectively, in consequence of the parallel nature of the chemical reaction and diffusion in porous solids.

Table 5
Effective diffusion coefficients of H_2SO_4 as a function of temperature (0.4 mol/L H_2SO_4, 10 g/L solids, stirring rate 480 rpm, particle size 75–53 μm)

Temperature °C	D_{eff} (cm^2/s)
30	1.7×10^{-7}
35	2.4×10^{-7}
40	3.1×10^{-7}
45	4.3×10^{-7}
50	6.3×10^{-7}
60	10.6×10^{-7}

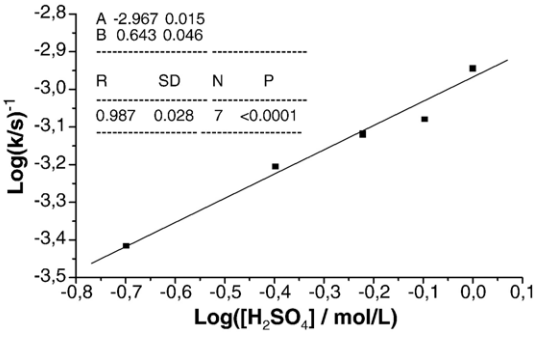

Fig. 10. Plot of k_D as a function of the sulphuric acid concentration.

Nomenclature

$[i]$	Molar concentration of species i
$[i]_s$	Molar concentration of species i at the outer surface of the particle
A	Surface area
b	Stoichiometric coefficient
D_{eff}	Effective diffusion coefficient
k	Chemical rate constant
k_0	Arrhenius pre-exponential factor
k_d	Apparent diffusion rate constant for non porous particles
k_D	Apparent diffusion rate constant according to the grain model
k_R	Apparent chemical reaction rate constant for non porous particles
n	Reaction order
r_i	Rate of reaction of species i
r_0	Initial particle radius
S_v	Surface area per unit volume
t^*	Grain model parameter
Zn. extr	Zinc extraction (%)
$[Zn]_{T_0}$	Initial zinc mass (g)
$[Zn]_{T_0+T}$	Solids zinc content (g) at T_{0+T}

Greek letters

α	Conversion
$\rho_{silicate}$	Silicate molar density
σ	Particle size parameter, dimensionless, see Eq. (8).
ε_0	Initial porosity of the solid (total pore volume (Table 2) × silicate density (4.0 g/cm$_3$))

Acknowledgements

This work was supported by Votorantim Metais Zinc, "FINANCIADORA DE ESTUDOS E PROJETOS — FINEP", and Universidade Federal de Ouro Preto-UFOP. The CAPES scholarship to P. S. Pina and the assistance of Mr. J. A. Magalhães and Ms. H. K. Reis, are gratefully acknowledged.

References

Abdel-Aal, E.A., 2000. Kinetics of sulphuric acid leaching of low-grade zinc silicate ore. Hydrometallurgy 55 (3), 247–254.

Aydogan, S., Aras, A., Canbazoglu, M., 2005. Dissolution kinetics of sphalerite in acidic ferric chloride leaching. Chemical Engineering Science 114, 67–72.

Bobeck, G.E., Su, H., 1985. The kinetics of dissolution of sphalerite in ferric chloride solutions. Metallurgical Transactions B 16, 413–424.

Bodas, M.G., 1996. Hydrometallurgical treatment of zinc silicate ore from Thailand. Hydrometallurgy 40 (1–2), 37–49.

Boni, M., 2005. The geology and mineralogy of non-sulphide zinc ore deposits. In: Umetsu, Y. (Ed.), Lead & Zinc '05. TMS, Warrendale, PA., Kyoto, Japan, pp. 1299–1313.

Chen, T., Dutrizac, J., 2003. Filter press plugging in zinc plant purification circuits. JOM, Journal of the Minerals, Metals and Materials Society 55 (4), 28–31.

Espiari, S., Rashchi, F., Sadrnezhad, S.K., 2006. Hydrometallurgical treatment of tailings with high zinc content. Hydrometallurgy 82 (1–2), 54–62.

Filippou, D., Konduru, R., Demopoulos, G.P., 1997. A kinetic study on the acid pressure leaching of pyrrhotite. Hydrometallurgy 47 (1), 1–18.

Gbor, P.K., Ahmed, I.B., Jia, C.Q., 2000. Behaviour of Co and Ni during aqueous sulphur dioxide leaching of nickel smelter slag. Hydrometallurgy 57 (1), 13–22.

Georgiou, D., Papangelakis, V.G., 1998. Sulphuric acid pressure leaching of a limonitic laterite: chemistry and kinetics. Hydrometallurgy 49 (1–2), 23–46.

Ghosh, M.K., Das, R.P., Biswas, A.K., 2002. Oxidative ammonia leaching of sphalerite Part I: non-catalytic kinetics. International Journal of Mineral Processing 66, 241–254.

Hua, Y., Lin, Z., Yan, Z., 2002. Application of microwave irradiation to quick leach of zinc silicate ore. Minerals Engineering 15 (6), 451–456.

Levenspiel, O., 1999. Chemical Reaction Engineering. John Wiley & Sons, New York. 664 pp.

Massaci, P., Recinella, M., Piga, L., 1998. Factorial experiments for selective leaching of zinc sulphide in ferric sulphate media. International Journal of Mineral Processing 53, 213–224.

Nzikou, J.M., Baklouti, M., Vincent, L.-M., Lapicque, F., 1997. Improvement in the measurement of diffusion coefficients in a restricted diffusion cell: case of binary electrolytes. Chemical Engineering and Processing 36 (2), 161–165.

Raghavan, S., Gajam, S.Y., 1986. Application of an enlarging pore model for the ammoniacal leaching of chrysocolla. Hydrometallurgy 16 (3), 271–281.

Ruiz, M.C., Padilla, R., 1998. Copper removal from molybdenite concentrate by sodium dichromate leaching. Hydrometallurgy 48 (3), 313–325.

Sahu, K.K., Agarwal, A., Pandey, B.D., 2005. Nickel recovery from spent nickel catalyst. Waste Management & Research 23, 148–154.

Silva, G., 2004. Relative importance of diffusion and reaction control during the bacterial and ferric sulphate leaching of zinc sulphide. Hydrometallurgy 73, 313–324.

Sohn, H.Y., Wadsworth, M.E., 1979. Rate Processes of Extractive Metallurgy. Plenum Press, New York. 472 pp.

Souza, A.D., 2000. Integration Process of the Treatments of Concentrates or Zinc Silicates ore and Roasted Concentrate of Zinc Sulphides.

Souza, A.D., Pina, P.S., Leao, V.A., 2007. Bioleaching and chemical leaching as an integrated process in the zinc industry. Minerals Engineering 20 (6), 591–599.

Szekely, J., Evans, J.W., Sohn, H.Y., 1976. Gas Solid Reactions. Academic Press, New York. 400 pp.

Terry, B., Monhemius, A.J., 1983. Acid dissolution of willemite ($(Zn, Mn)_2SiO_4$) and hemimorphite ($Zn_4Si_2O_7(OH)_2H_2O$). Metallurgical Transactions B, Process Metallurgy 14 (3), 335–346.

Umino, S., Newman, J., 1997. Temperature dependence of the diffusion coefficient of sulphuric acid in water. Journal of the Electrochemical Society 144 (4), 1302–1307.

Zhou, H.-m., Zheng, S.-l., Zhang, Y., Yi, D.-q., 2005. A kinetic study of the leaching of a low-grade niobium–tantalum ore by concentrated KOH solution. Hydrometallurgy 80 (3), 170–178.